# Spectroscopic and Hydrodynamic Studies Reveal Structural Differences in Normal and Transforming H-ras Gene Products†

Alfred Pingoud,* Matthias Wehrmann, Uwe Pieper, Frank-Ulrich Gast, Claus Urbanke, Jürgen Alves, Jürgen Feuerstein,‡ and Alfred Wittinghofer‡

*Zentrum Biochemie, Medizinische Hochschule Hannover, Konstanty-Gutschow-Strasse 8, D-3000 Hannover 51, West Germany*

*Received November 23, 1987; Revised Manuscript Received February 23, 1988*

ABSTRACT: We have recorded the circular dichroism spectra of the cellular and the viral H-ras gene products both in the absence and in the presence of guanine nucleotides and analyzed these spectra in terms of the secondary structure composition of these proteins. It is shown that the GTP complex of the ras proteins has a different secondary structure composition than the GDP complex and, furthermore, that there are differences in the secondary structure of the viral ras protein and the cellular ras protein. We have also recorded and analyzed the circular dichroism spectrum of the isolated guanine nucleotide binding domain of the *Escherichia coli* elongation factor Tu (EF-Tu), which has been considered as a model for the tertiary structure of the ras proteins [McCormick, F., Clark, B. F. C., LaCour, T. F. M., Kjeldgaard, M., Norskov-Lauritsen, L., & Nyborg, J. (1985) *Science* (*Washington, D.C.*) *230*, 78–82]. Our data show that the guanine nucleotide binding domain of EF-Tu (30% $\alpha$-helix and 16% $\beta$-pleated sheet for the GDP complex) has quite a different secondary structure composition than the ras proteins (e.g., the cellular ras protein has 47% $\alpha$-helix and 22% $\beta$-pleated sheet for the GDP complex), indicating that the protein core comprising the guanine nucleotide binding site might be similar but that major structural differences must exist at the portion outside this core. Normal and transforming ras proteins also differ slightly in their hydrodynamic properties as shown by sedimentation velocity runs in the analytical ultracentrifuge. The cellular ras protein has an $s_{20,w}$ value of 2.4 S and the viral homologue has an $s_{20,w}$ value of 2.2 S, indicating that the former is somewhat more compact than the latter. The structural differences between the cellular and the viral ras proteins do not affect the stability of these proteins toward guanidinium chloride induced or temperature-induced denaturation, as shown by circular dichroism spectroscopy and GDP exchange activity measurements.

The ras gene family in humans consists of at least three genes, H-ras, K-ras, and N-ras, which are involved in a variety of human tumours [for a recent review, cf. Barbacid (1987)]. They encode proteins of a molecular weight of 21 000 (Shih et al., 1979), designated p21, which bind guanine nucleotides with high affinity (Shih et al., 1980) and hydrolyze GTP (Gibbs et al., 1984; McGrath et al., 1984; Sweet et al., 1984). Their mechanism of action, despite extensive efforts, is still unknown. The amino acid sequence of the ras proteins shows considerable homologies with other guanine nucleotide binding proteins, in particular the ras-related yeast proteins RAS1, RAS2, YPT1, rho, and SEC4, but also with the elongation and initiation factors of protein synthesis, the *Escherichia coli* lepA and era proteins, tubulin and the $\alpha$-subunit of the G protein family, $G_s$, $G_i$, $G_o$, transducin, etc. (Halliday, 1984; Leberman & Egner, 1984; Lochrie et al., 1985; Dever et al., 1987).

The homology between the *E. coli* elongation factor Tu (EF-Tu) and the ras proteins is of particular interest, since this protein has been studied extensively with respect to structure and mechanism. EF-Tu is the only guanine nucleotide binding protein for which the X-ray structure of its guanine nucleotide binding domain is known (Jurnak, 1985; LaCour et al., 1985). EF-Tu is also one of the few guanine nucleotide binding proteins for which precise information exists as to the correlation between guanine nucleotide binding and hydrolysis on one side and its function on the other side (Kaziro, 1978; Bosch et al., 1983; Parmeggiani & Swart, 1985).

By analogy to guanine nucleotide binding proteins involved in signal transduction [for recent reviews cf. Stryer and Bourne (1986) and Gilman (1987)], it is believed that the binding and hydrolysis of GTP are involved in the regulation of the active and inactive states of ras proteins. Guanine nucleotides are considered to be allosteric effectors for the conformational transition between these two states. It is generally assumed that a disturbance of GTP binding and hydrolysis as well as GDP/GTP exchange alters the steady-state distribution of these states and thereby affects the physiological response in which ras proteins are involved.

Although the target molecules with which ras proteins interact have not yet been identified, it is reasonable to assume that the regulation of such interactions is dependent on a transition between active and inactive conformations of the ras proteins. We have been interested to find out whether structural differences can be detected between ras proteins complexed with GDP or GTP and the normal cellular and transforming ras proteins. Circular dichroism spectroscopy and analytical ultracentrifugation were chosen for this investigation, because they yield directly structural information, namely, secondary structure composition and Stokes radii.

## Experimental Procedures

*Proteins.* The H-ras protooncogene product c-p21, the viral H-ras oncogene product v-p21 (Arg-12, Thr-59) (Dahr et al., 1982), and the H-ras oncogene product derived from a human bladder carcinoma t-p21 (Val-12) (Reddy et al., 1982; Tabin

† This paper is dedicated to Prof. F. Schneider on the occasion of his 60th birthday. This work was supported by the Deutsche Forschungsgemeinschaft (Pi 122/3-2) and the Fonds der Chemischen Industrie.

‡ Present address: Max-Planck-Institut für Medizinische Forschung, Jahnstrasse 29, D-6900 Heidelberg, West Germany.

0006-2960/88/0427-4735$01.50/0 

et al., 1982; Taparowsky et al., 1982) were isolated as guanine nucleotide (mainly GDP) complexes from *E. coli* RRIΔM15 transformed with a plasmid harboring the H-ras gene under the control of the tac promoter as described recently (Tucker et al., 1986). They were stored in 50 mM tris(hydroxymethyl)aminomethane hydrochloride (Tris-HCl) pH 7.5, 5 mM $MgCl_2$, 1 mM 1,4-dithioerythritol, and 0.1 μM GDP at −70 °C. Immediately prior to the experiment they were subjected to high-performance liquid chromatography (HPLC) on a 21.5 × 150 mm TSK-phenyl-5PW column (Beckman Instruments) as described (Feuerstein et al., 1987) in order to obtain the nucleotide-free proteins.

The guanine nucleotide binding domain (G domain) of EF-Tu was isolated from *E. coli* TGE 900 transformed with a plasmid harboring a mutated tufA gene under the control of the $p_L$ promoter. In brief, the mutation was introduced by cleaving the tufA gene with the Asp-718 restriction endonuclease at codon 224, followed by a fill-in reaction with Klenow polymerase and religation. Details of this construction will be published elsewhere. This yields a mutant tufA gene coding for the N-terminal domain of EF-Tu, i.e., amino acids 1–225 plus five additional amino acids introduced as a consequence of the tail to tail religation. Isolation of the genetically engineered G domain of EF-Tu was carried out similarly as described for a nearly identical EF-Tu mutant (Parmeggiani et al., 1987), substituting the Mono Q with hydroxyapatite chromatography.

*High-Performance Liquid Chromatography Analysis of Guanine Nucleotides.* HPLC of guanine nucleotide containing samples was performed at ambient temperature on a Merck-Hitachi 655 A-12 HPLC system using a 4 × 250 mm RP-18 column (Merck, Darmstadt). Isocratic elution was carried out with 50 mM potassium phosphate, pH 5.9, 2 mM tetrabutylammonium hydrogen phosphate, and 12% v/v acetonitrile at a flow rate of ~1 mL/min resulting in a back pressure of ~100 bar. Under these conditions protein-bound guanine nucleotides are released and are coeluted with free guanine nucleotides in the order GMP, GDP, and GTP (Block & Pingoud, 1981).

*Circular Dichroism Spectroscopy.* All spectroscopic experiments were carried out in 50 mM Tris-HCl, pH 7.5, 5 mM $MgCl_2$, and 1 mM 1,4-dithioerythritol.

Circular dichroism spectra were recorded at 0 °C in 1-mm cuvettes in a Jobin-Yvon Dichrograph R. J. Mark III calibrated with (+)-camphor-10-sulfonic acid, D-pantolactone, and epiandrosterone. The bandwidth was 2 nm, the rate of scanning was 0.02 nm/s, and the time constant was 10 s. Spectra were stored in a digital recorder, processed, and analyzed numerically in terms of α-helix, β-pleated sheet, and residual structure content similarly as described by Chen et al. (1972) with myoglobin, lysozyme, lactate dehydrogenase, papain, and ribonuclease A as reference proteins. Figure 1 shows the experimental and computed circular dichroism spectrum of the c-p21–GDP complex.

*Analytical Ultracentrifugation.* All hydrodynamic experiments were carried out in 50 mM Tris-HCl, pH 7.5, 5 mM $MgCl_2$, 1 mM 1,4-dithioerythritol, and 0.1 μM GDP. Sedimentation velocity runs were performed at 20 °C in 12-mm cells in an An-F-Ti-rotor at 60000 rpm in a Spinco Model E analytical ultracentrifuge equipped with an electronic speed control, a high-intensity ultraviolet-illumination system, a photoelectric scanner, and an electronic multiplexer. Sedimentation profiles were recorded at 280 nm, stored in a digital recorder, and used for the evaluation of the $s_{20,w}$ value for c-, v-, and t-p21–GDP.

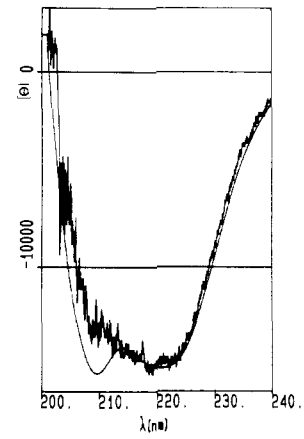


FIGURE 1: Circular dichroism spectrum of c-p21–GDP. The spectrum of 0.22 mg/mL c-p21–GDP was recorded with a sensitivity of 5 × $10^{-6}$. Superimposed on the experimental [θ] vs λ curve is the computed spectrum for a protein with 47% α-helix, 22% β-pleated sheet, and 31% residual structure.

*Denaturation Studies.* Denaturation of p21–GDP was induced by addition of variable amounts of guanidinium hydrochloride and incubation for 15 min, if not otherwise stated, at 20 °C. Unfolding was measured by recording the circular dichroism at 220 nm. The [$^3$H]GDP/GDP exchange activity was determined in parallel by addition of 2 μL of a 11.3 Ci/mmol [$^3$H]GDP (Amersham-Buchler) solution to a 20-μL sample. Final concentrations were 70 μM p21–GDP and 2 μM [$^3$H]GDP. After 15 min at 25 °C, the radioactivity retained on a nitrocellulose filter (Sartorius, type 11306) was measured in a scintillation counter.

The temperature-induced denaturation of c- and v-p21 was also studied by recording the circular dichroism at 220 nm. For this purpose, a Haake thermostat was used. The temperature increase per time was ~30 °C/h and identical in all experiments.

## RESULTS

Hydrophobic interaction chromatography on a TSK-phenyl-5PW column was used to prepare nucleotide-free c-p21, v-p21, and t-p21. The removal of the nucleotides was checked by UV absorption spectroscopy and high-performance liquid chromatography (Block & Pingoud, 1981). The TSK-phenyl-5PW chromatography also removes residual protein impurities, in particular a partially degraded p21 which in variable amounts is copurified from *E. coli* extracts and is detected on sodium dodecyl sulfate–polyacrylamide gel electrophoretic (SDS–PAGE) gels as a band migrating slightly faster than authentic p21. All the experiments reported here were carried out with HPLC-purified p21, which shows one sharp band on SDS–PAGE gels.

*Circular Dichroism.* Circular dichroism spectra of c-p21, v-p21, and t-p21 were recorded either in the absence or in the presence of GTP or GDP. The spectra of the nucleotide-free p21 were recorded immediately after the chromatographic separation, because p21 is rather unstable in the absence of nucleotides. Subsequently, GTP was added in stoichiometric amounts and the circular dichroism measured to obtain the p21–GTP spectrum. Given the high affinity of p21 to guanine nucleotides, the amount of added GTP was sufficient to convert p21 into the p21–GTP complex. On the other hand, the resulting concentration of GTP was so low that no base-line correction for the circular dichroism of the GTP moiety was needed. Twenty-four hours after the p21–GTP spectrum had been recorded, a sufficient time interval to allow for complete GTP hydrolysis under these conditions, as shown by high-

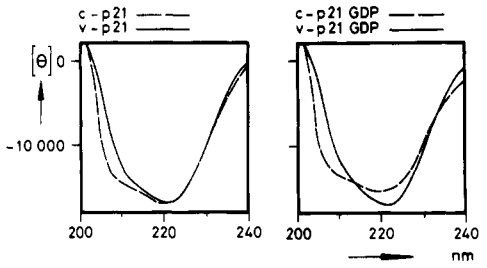


FIGURE 2: Circular dichroism spectra of c-p21 and v-p21 in the absence or presence of GDP.

performance liquid chromatography, the circular dichroism spectrum was recorded again. The p21–GDP spectrum was compared with the spectrum obtained after direct addition of a stoichiometric amount of GDP to freshly prepared nucleotide-free p21 and found to be identical.

Figure 2 shows the circular dichroism spectra of nucleotide-free c-p21, and of the c-p21–GDP complex. The spectra of nucleotide-free c-p21 and c-p21–GTP (not shown) are almost identical, while the c-p21–GDP spectrum is slightly different from the c-p21 and c-p21–GTP spectra. From the rate of the intrinsic GTPase activity of c-p21, $k_{cat} = 5 \times 10^{-4}$ $s^{-1}$ measured under these conditions at 37 °C (J. Feuerstein and F. U. Gast, unpublished data), it can be inferred that the c-p21–GTP complex is stable for sufficient time to record the circular dichroism spectrum at 0 °C. This was verified experimentally by high-performance liquid chromatography. Using this technique, it was also shown that c-p21–GTP cannot be obtained in pure form by incubating c-p21–GDP with phosphoenolpyruvate and pyruvate kinase presumably due to the relatively fast GTPase reaction and the slow exchange of GDP for GTP.

Figure 2 shows also the circular dichroism spectra of nucleotide-free v-p21, and of the v-p21–GDP complex. The nucleotide-free v-p21 and v-p21–GTP (not shown) spectra are identical within experimental error and similar to, albeit not identical with the corresponding c-p21 spectra. The nucleotide composition of the samples was checked by high-performance liquid chromatography. In agreement with the lower intrinsic GTPase of v-p21, $k_{cat} = 0.4\ (\pm 0.1) \times 10^{-4}$ $s^{-1}$ at 37 °C (J. Feuerstein and F. U. Gast, unpublished data), v-p21–GTP is stable at 0 °C for considerable time. Incubation at 25 °C for 24 h is necessary to hydrolyze most of the GTP to GDP. The v-p21–GDP spectrum obtained after hydrolysis of v-p21–GTP is identical with the one obtained after addition of GDP to nucleotide-free v-p21.

We have also measured the circular dichroism of t-p21 in the presence and absence of guanine nucleotides. The spectra of the nucleotide-free t-p21 and the t-p21–GTP complex resemble those of v-p21. The effect of GDP binding on the t-p21 spectrum, however, is not quite as pronounced as that with c-p21 or v-p21 (spectra not shown, but see Table I).

The circular dichroism spectra of c-, v-, and t-p21 were analyzed in terms of their secondary structure composition essentially as described by Chen et al. (1972). The c-p21–GDP spectrum was also evaluated by the method of Provencher and Glöckner (1981). Both procedures gave a reasonably good fit between experimental and calculated curves (cf. Figure 1). Deviations between experimental and computed circular dichroism spectra of p21 indicate that p21 contains several short $\alpha$-helices which differ from long $\alpha$-helices in showing a larger negative ellipticity at 220 nm than at 210 nm (Chen et al., 1974). Since $\beta$-pleated sheets and even more so $\beta$-turns have a much broader range of conformation than $\alpha$-helices, it is also possible that p21 contains $\beta$-pleated sheets and $\beta$-turns which

Table I: Secondary Structure Compositon of c-p21, v-p21, and t-p21 in the Presence and Absence of GDP or GTP[a]

| | % $\alpha$-helix | % $\beta$-sheet | % residual structure |
|---|---|---|---|
| c-p21 | 56 ± 5 (55) | 25 ± 3 (27) | 19 ± 5 (18) |
| c-p21–GTP | 54 ± 5 | 23 ± 3 | 23 ± 5 |
| c-p21–GDP | 47 ± 5 | 22 ± 3 | 31 ± 5 |
| v-p21 | 52 ± 5 | 18 ± 3 | 29 ± 5 |
| v-p21–GTP | 52 ± 5 | 18 ± 3 | 29 ± 5 |
| v-p21–GDP | 39 ± 5 | 18 ± 3 | 41 ± 5 |
| t-p21 | 52 ± 5 | 15 ± 3 | 33 ± 5 |
| t-p21–GTP | 51 ± 5 | 16 ± 3 | 34 ± 5 |
| t-p21–GDP | 46 ± 5 | 18 ± 3 | 36 ± 5 |
| G-domain–GDP | 30 ± 5 | 16 ± 3 | 54 ± 5 |

[a] All circular dichroism spectra were analyzed by the method of Chen et al. The c-p21 spectrum was also analyzed by the Provencher and Glöckner procedure: the result is given in parentheses. The estimate of the accuracy of the secondary structure analysis is based on the results of several independent experiments.

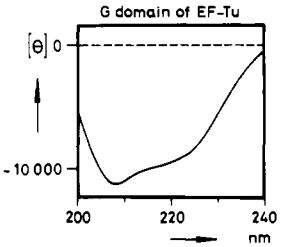


FIGURE 3: Circular dichroism spectrum of the guanine nucleotide binding domain of the *E. coli* elongation factor Tu in the presence of GDP.

are not sufficiently well represented by the set of reference proteins used here to give a more precise fit between experimental and calculated spectra as obtained here (Yang et al., 1986). The results of the numerical analyses of the spectra are given in Table I.

The structure of the guanine nucleotide binding domain of the *E. coli* elongation factor Tu has been considered as a model for the structure of other guanine binding proteins (McCormick et al., 1985; Cenatiempo et al., 1987). In order to verify the validity of such tertiary structure predictions for ras proteins, we have isolated the genetically engineered G-domain and recorded its circular dichroism spectrum (Figure 3). It can be seen that the GDP complex of the G-domain of EF-Tu gives a different spectrum than c-p21 or v-p21. The secondary structure analysis shows that the G-domain contains much less $\alpha$-helical regions than the ras proteins (Table I).

*Analytical Ultracentrifugation.* In order to find out whether the structural difference between c-p21 and v-p21 detected by circular dichroism spectroscopy is also apparent in hydrodynamic investigations, we have carried out sedimentation velocity runs in the analytical ultracentrifuge. Because of the small amounts of HPLC-purified ras proteins available and the relative instability of p21 in the nucleotide-free form, only the GDP complex of c-p21 and v-p21 was studied. Figure 4 shows the result of an experiment in which the sedimentation of c-p21–GDP and v-p21–GDP was analyzed in the same run. This is mandatory for the determination of small differences in $s$ value, as expected for c-p21 and v-p21.

From this experiment an $s_{20,w}$ value of 2.4 S was determined for c-p21–GDP and 2.2 S for v-p21–GDP, corresponding to Stokes radii of 19.9 and 21.5 Å, respectively (Table II). Similar results were obtained with p21 preparations which were electrophoretically more than 95% pure but had not been subjected to the TSK-phenyl-6PW chromatography. In one experiment with such material, t-p21–GDP ($s_{20,w}$ = 2.02 S) was shown to sediment more slowly than v-p21–GDP ($s_{20,w}$

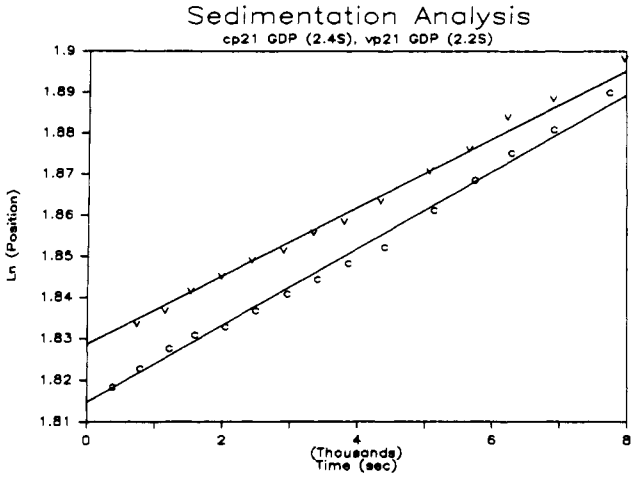


FIGURE 4: Analysis of sedimentation velocity runs of c-p21–GDP and v-p21–GDP. Sedimentation velocity runs were carried out with 0.53 mg/mL c-p21–GDP and v-p21–GDP. Sedimentation profiles were evaluated for the position of the boundary. From the half-logarithmic plot, $s$ values of 2.4 S and 2.2 S were determined for c-p21–GDP (c) and v-p21–GDP (v), respectively.

Table II: Hydrodynamic Parameters of the GDP Complexes of c-p21, v-p21, and t-p21[a]

| | $s_{20,w}$ (S) | Stokes radius (Å) |
|---|---|---|
| c-p21–GDP | 2.4 (±0.05) | 19.9 |
| v-p21–GDP | 2.2 (±0.05) | 21.5 |
| t-p21–GDP | 2.0 (±0.05) | 23.6 |

[a] The c-p21 and v-p21 data were obtained with HPLC-purified p21 and the t-p21 data with conventionally purified material (see text).

= 2.25 S) and c-p21–GDP ($s_{20,w}$ = 2.4 S). Analytical ultracentrifuge runs were carried out only at one concentration (0.53 mg/mL). Since the sedimentation coefficients were determined in dilute solution, it is assumed that they are the same as those extrapolated to zero concentration, if measurements at different concentrations had been made.

*Denaturation Studies.* The substitution in p21 of one (t-p21) or two (v-p21) amino acids which influence structural parameters of the ras proteins might also have an effect on their structural stability. We have analyzed, therefore, the guanidinium chloride induced as well as the temperature-induced denaturation of c-p21 and v-p21. Figure 5 shows the dependence of the secondary structure composition of v-p21 on the guanidinium chloride concentration, as measured by the circular dichroism of these proteins. In parallel, the GDP binding activity was determined. It can be shown that the decrease in ordered structure induced by guanidinium chloride is accompanied by a concomitant loss of GDP binding activity. Similar experiments with c-p21 (not shown) demonstrate that there is no difference in the sensitivity of c-p21–GDP and v-p21–GDP toward guanidinium chloride induced denaturation. It was noticed, however, that the denaturation of v-p21–GDP was readily reversible upon removal of guanidinium chloride, while partially denatured c-p21–GDP precipitated after incubation for several hours at 25 °C.

Temperature-induced denaturation profiles of c-p21–GDP and v-p21–GDP are shown in Figure 6. These "melting" curves were recorded under identical conditions, in particular with the same rate of heating, and are identical within the limits of error.

## Discussion

The similarity of ras proteins with the $\alpha$-subunit of G proteins has led to the proposal that ras proteins are involved

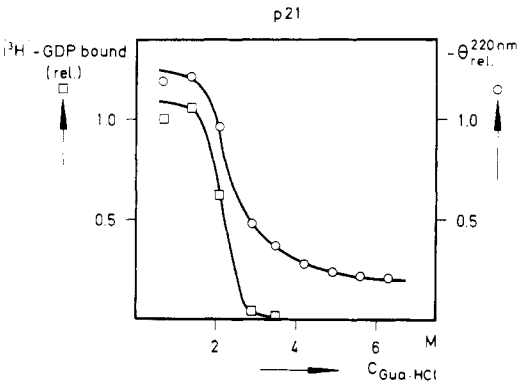


FIGURE 5: Guanidinium chloride induced unfolding of v-p21–GDP. v-p21–GDP (1.67 mg/mL) was exposed to increasing amounts of guanidinium chloride. The effect of unfolding was studied by measuring the change in ellipticity at 220 nm (○) as well as the [$^3$H]GDP/GDP exchange activity (□). Within the limits of error, identical curves were obtained for c-p21–GDP.

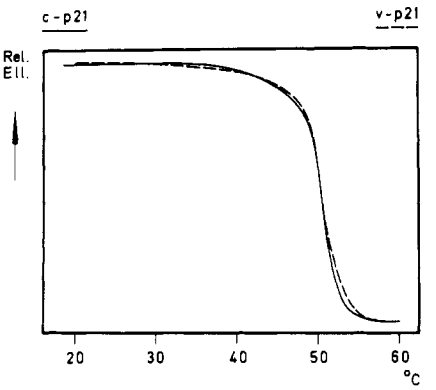


FIGURE 6: Thermal unfolding of c-p21–GDP and v-p21–GDP. The change in ellipticity at 220 nm of 0.56 mg/mL c-p21–GDP (—) or v-p21–GDP (– –) was continuously recorded while increasing the temperature at a defined rate from 20 to 60 °C.

in signal transduction (Gilman, 1984). They are considered to adopt two conformations, an inactive one, when GDP is bound, and an active one, when GTP is bound. The exchange of GDP for GTP is thought to occur in response to an as yet unidentified, possibly external stimulus, which in turn is passed on to a putative effector molecule, presumably an enzyme, which amplifies the original signal. Deactivation could be achieved by the intrinsic GTPase activity of the ras proteins. Mutant ras proteins with altered affinity to guanine nucleotides or reduced GTPase activity according to this model would interfere with the steady-state distribution between active and inactive conformations and thereby disturb the regular signal transduction process. Indeed, transforming mutant ras proteins have been identified with reduced GTPase activity as well as altered affinity for GDP and GTP. It is conceivable, furthermore, that mutations might lead to a constitutively activated ras protein, which is not dependent on GTP to adopt the active conformation. As a matter of fact, mutant ras proteins have been described that do not bind guanine nucleotides with measurable affinity but nevertheless are transforming (Walter et al., 1986; Der et al., 1986; Clanton et al., 1987). Central to this model of the mechanism of action of normal and transforming ras proteins is the idea of a different conformation of ras proteins in the GDP and the GTP state. Such differences in conformation, however, have as yet not been reported. Also, there are at present no data available which demonstrate conformational differences between normal and mutant ras proteins, other than the observation that some mutant ras proteins have an altered electrophoretic mobility

in the presence of sodium dodecyl sulfate (Cooper & Lane, 1983; Shih, 1984; Seeburg et al., 1984; Fasano et al., 1984; Temeles et al., 1985; Tucker et al., 1986). There are several reports, however, in which on the basis of energy calculations (Pincus et al., 1983), or secondary structure predictions (Santos et al., 1983; Seeburg et al., 1984), conformational differences between c-p21 and v-p21, as well as other transforming p21 proteins, have been postulated.

In the present paper we have shown that differences in the circular dichroism exist between p21 in the GTP form and p21 in the GDP form. These differences are not large, but are reproducibly obtained with homogeneous preparations of p21 and a carefully calibrated circular dichroism spectrophotometer. The fact that these differences are obtained within one experiment in which advantage is taken of the p21-catalyzed conversion of GTP to GDP lends credit to the significance of this observation. It is shown, furthermore, that nucleotide-free p21 has an identical circular dichroism with p21–GTP. It can, therefore, be assumed that binding of GTP does not significantly alter the conformation of p21 and that the hydrolysis of GTP to GDP, however, does induce a conformational transition in ras proteins. Differences in the circular dichroism are also apparent when one compares c-p21, v-p21, and t-p21. The largest differences are seen between c-p21–GDP and v-p21–GDP.

Circular dichroism spectroscopy offers the possibility to relate spectroscopic and structural parameters. With polypeptides or proteins of known secondary structure, it is possible to derive reference spectra for $\alpha$-helix, $\beta$-pleated sheet, and other structures (Greenfield & Fasman, 1969; Saxena & Wetlaufer, 1971) and to use these in turn to get an estimate of the secondary structure composition of a protein whose circular dichroism spectrum is known. It should be emphasized that this is an empirical procedure, which in general gives satisfactory results but also has limitations. As pointed out by Yang et al. (1986), the analysis of a circular dichroism spectrum with a well-defined double minimum at 222 and 208–210 nm or a single minimum between 210 and 220 nm can be accepted with considerable confidence. On the other hand, if the circular dichroism bands between 200 and 240 nm are broad, or skewed or have shoulders, as with p21, the secondary structure estimates are more uncertain. We emphasize, therefore, the qualitative differences between the circular dichroism spectra of c-p21, v-p21, and t-p21 in the absence or presence of GDP or GTP. These differences can be due to a change of the secondary structure composition as summarized in Table I but could be attributable also to alterations in aromatic side chain contributions, to changes in helix parameters, and to protein aggregation (as was pointed out by a reviewer of this paper). p21 is of similar size as the guanine nucleotide binding domain of EF-Tu with which it shares considerable sequence homology. This has led McCormick et al. (1985) to propose a structural model for the tertiary structure of p21. The model was constructed by substituting homologous sequences of p21 in the EF-Tu structure, which is known from X-ray analyses. The degree of success expected in the prediction of related structures depends on the degree of sequence homology. Lesk and Chotia (1986) suggest that related structures can only provide useful models of closely related proteins if the homology is greater than about 50%. This is not the case for p21 and EF-Tu. In order to test the validity of the tertiary structure model of p21 proposed by McCormick et al., we have, therefore, compared the secondary structure composition of p21 and that of the genetically engineered G-domain of EF-Tu. This comparison shows that the G-domain has a rather different secondary structure than p21. It is premature to conclude from this result that the two proteins are dissimilar in structure. We suggest, however, on the basis of our data that similarities are restricted to the protein core, i.e., the guanine nucleotide binding site, and that the portion outside this core will differ substantially in structure.

The differences in secondary structure composition of c-p21 and v-p21 are sufficiently large that one would expect the overall shape of these proteins to be different. This is indeed the case: hydrodynamic studies show that c-p21–GDP is more compact than v-p21–GDP and t-p21–GDP, confirming a prediction of Santos et al. (1983) which was based on secondary structure considerations.

In spite of these structural differences, there is no pronounced difference in stability to thermal and chemical denaturation between c-p21–GDP and v-p21–GDP. Guanidinium chloride induced denaturation of c-p21 and v-p21 reveals, however, a stronger tendency of c-p21–GDP as compared to v-p21–GDP to aggregate upon long-time incubation with the denaturating agent.

In conclusion, our results support the current model for the mechanism of action of ras proteins which proposes that ras proteins can adopt two conformations which are stabilized by GDP or GTP, respectively, and which are different or differently populated with normal and transforming ras proteins.

## ACKNOWLEDGMENTS

We are indebted to Dr. H.-J. Ehbrecht for an *E. coli* clone containing the truncated tufA gene. We thank Dr. F. Jurnak and Dr. M. Kjeldgaard for helpful discussions, Dr. G. Maass for his interest and support, Dr. F. Peters and K. Stieglitz for their assistance in the numerical analysis of circular dichroism spectra, Dr. S. W. Provencher for supplying computer programs, and Dr. J. Potel for making laboratory facilities available to us. We gratefully acknowledge the expert technical assistance of R. Mull. We thank T. Rueter for critical reading of the manuscript and E. Schuchardt for typing the manuscript.

## REFERENCES

Barbacid, M. (1987) *Annu. Rev. Biochem. 56*, 779–827.

Block, W., & Pingoud, A. (1981) *Anal. Biochem. 114*, 112–117.

Bosch, L., Kraal, B., Van der Meide, P. H., Duisterwinkel, F. J., & Van Noort, J. M. (1983) *Prog. Nucleic Acid Res. Mol. Biol. 30*, 91–126.

Cenatiempo, Y., Deville, F., Doudon, J., Grunberg-Manago, M., Sacerdot, C., Hershey, J. W. B., Hansen, H. F., & Petersen, H. U. (1987) *Biochemistry 26*, 5070–5076.

Chen, Y.-H., Yang, J. T., & Martinez, H. M. (1972) *Biochemistry 11*, 4120–4131.

Chen, Y.-H., Yang, J. T., & Chau, K. H. (1974) *Biochemistry 13*, 3350–3361.

Clanton, D. J., Lu, Y., Blair, D. G., & Shih, T. Y (1987) *Mol. Cell. Biol. 7*, 3092–3097.

Clark, B. F. C. Kjeldgaard, M., LaCour, T. F. M., Mortensen, K. K., & Nyborg, J. (1987) *Biochemistry 26*, 5070–5076.

Cooper, G. M., & Lane, M. A. (1983) *Biochim. Biophys. Acta 738*, 9–20.

Der, C. J., Pan, B.-T. & Cooper, G. M. (1986) *Mol. Cell. Biol. 6*, 3291–3294.

Dever, T. E., Glynias, M. J., & Merrick, W. C. (1987) *Proc. Natl. Acad. Sci. U.S.A. 84*, 1814–1818.

Dhar, R., Ellis, R. W., Shih, T. Y., Oroszlau, S., Shapiro, B., Maizel, J., Lowry, D., & Scolnick, E. (1982) *Science*

(*Washington, D.C.*) *217*, 934–937.
Fasano, O., Aldrich, T., Tamanoi, F., Taparowsky, E., Furth, M., & Wigler, M. (1984) *Proc. Natl. Acad. Sci. U.S.A. 81*, 4008–4012.
Feig, L. A., Pan, B. T., Roberts, T. M., & Cooper, G. M. (1986) *Proc. Natl. Acad. Sci. U.S.A. 83*, 4607–4611.
Feuerstein, J., Goody, R. S., & Wittinghofer, A. (1987) *J. Biol. Chem. 262*, 8455–8458.
Gibbs, J. B., Sigal, I. S., Poe, M., & Scolnick, E. M. (1984) *Proc. Natl. Acad. Sci. U.S.A. 81* 5704–5708.
Gilman, A. G. (1984) *Cell* (*Cambridge, Mass.*) *36*, 577–579.
Gilman, A. G. (1987) *Annu. Rev. Biochem. 56*, 615–649.
Greenfield, N., & Fasman, G. D. (1969) *Biochemistry 8*, 4108–4116.
Halliday, K. (1984) *J. Cyclic Nucleotide Protein Phosphorylation Res. 9*, 435–448.
Jurnak, F. (1985) *Science 230*, 32–36.
Kaziro, Y. (1978) *Biochim. Biophys. Acta 505*, 95–127.
LaCour, T. F. M., Nyborg, J., Thirup, S., & Clark, B. F. C. (1985) *EMBO J. 4*, 2385–2388.
Leberman, R., & Egner, U. (1984) *EMBO J. 3*, 339–341.
Lesk, A. M., & Chothia, C. H. (1986) *Philos. Trans. R. Soc. London A. 317*, 345–356.
Lochrie, M. A., Hurley, J. B., & Simon, M. I. (1985) *Science* (*Washington, D.C.*) *228*, 96–99.
McCormick, F., Clark, B. F. C., LaCour, T. F. M., Kjeldgaard, M., Norskov-Lauritsen, L., & Nyborg, J. (1985) *Science* (*Washington, D.C.*) *230*, 78–82.
McGrath, J. P., Capon, D. J., Goeddel, D. V., & Levinson, A. D. (1984) *Nature* (*London*) *310*, 644–649.
Parmeggiani, A., & Swart, G. W. M. (1985) *Annu. Rev. Microbiol. 39*, 557–577.
Parmeggiani, A., Swart, G. W. M., Mortensen, K. K., Jensen, M., Clark, B. F. C., Dente, L., & Cortese, R. (1987) *Proc. Natl. Acad. Sci. U.S.A. 84*, 3141–3145.
Pincus, M. R., van Renswoude, J., Harford, J. B., Chang, E. H., Carty, R. P., & Klausner, R. D. (1983) *Proc. Natl. Acad. Sci. U.S.A. 80*, 5253–5257.
Provencher, S. W., & Glöckner, J. (1981) *Biochemistry 20*, 33–42.
Reddy, E. P., Reynolds, R. K., Santos, E., & Barbacid, M. (1982) *Nature* (*London*) *300*, 149–152.
Santos, E., Reddy, E. P., Pulciani, S., Feldman, R. J., & Barbacid, M. (1983) *Proc. Natl. Acad. Sci. U.S.A. 80*, 4679–4683.
Saxena, V. P., & Wetlaufer, D. B. (1971) *Proc. Natl. Acad. Sci. U.S.A. 68*, 969–972.
Seeburg, P. H., Colby, W. W., Capon, D. J., Goeddel, D. V., & Levinson, A. D. (1984) *Nature* (*London*) *312*, 71–75.
Shih, T. Y. (1984) *Cancer, Invest. 2*, 109–123.
Shih, T. Y., Weeks, M. O., Young, H. A., & Scolnick, E. M. (1979) *Virology 96*, 64–79.
Shih, T. Y., Papageorge, A., Stokes, P. E., Weeks, M. O., & Scolnick, E. M. (1980) *Nature* (*London*) *287*, 686–691.
Stryer, L., & Bourne, H. R. (1986) *Annu. Rev. Cell Biol. 2*, 391–420.
Sweet, R. W., Yokoyama, S., Kamata, T., Feramisco, J. R., Rosenberg, M., & Gross, M. (1984) *Nature* (*London*) *311*, 273–275.
Tabin, C. J., Bradley, S. M., Bargmann, C. I., Weinberg, R. A., Papageorge, A. G., Scolnick, E. M., Dhar, R., Lowy, D. R., & Chang, E. H. (1982) *Nature* (*London*) *300*, 143–148.
Taparowsky, E., Suard, Y., Fasano, O., Shimizu, K., Goldfarb, M., & Wigler, M. (1982) *Nature* (*London*) *300*, 762–765.
Temeles, G. L., Gibbs, J. B., D'Alonzo, J. S., Sigal, J. S., & Scolnick, E. M. (1985) *Nature* (*London*) *313*, 700–703.
Tucker, J., Sczakiel, G., Feuerstein, J., John, J., Goody, R. S., & Wittinghofer, A. (1986) *EMBO J. 5*, 1351–1358.
Walter, M., Clark, S. G., & Levinson, A. D. (1986) *Science* (*Washington, D.C.*) *233*, 649–652.
Yang, J. T., Wu, C.-S. C., & Martinez, H. M. (1986) *Methods Enzymol. 130*, 208–269.